

Distortion and Charge Density Wave in the Ga Square Net Coupled to the Site Occupancy Wave in $\text{YCo}_{0.88}\text{Ga}_3\text{Ge}$

Danielle L. Gray, Melanie C. Francisco, and Mercouri G. Kanatzidis*

Department of Chemistry, Northwestern University, Evanston, Illinois 60208

Received April 4, 2008

$\text{YCo}_{0.88}\text{Ga}_3\text{Ge}$ has an incommensurately modulated structure that was solved with $(3 + 1)\text{D}$ superspace techniques. $\text{YCo}_{0.88}\text{Ga}_3\text{Ge}$ crystallizes in the orthorhombic superspace group $Immm(\alpha 00)00s$ with unit cell constants of $a = 4.1639(4)$, $b = 4.1639(4)$, $c = 23.541(2)$ Å and a modulation vector of $q = 0.3200(4)a^*$ at 293 K. The incommensurate modulation, which creates a very large supercell (~ 25 fold), arises from a charge density wave (CDW) in the square net of Ga atoms that is coupled with a site occupancy wave (SOW) of Co atoms. The distorted Ga net features polygallide ribbons, chains, as well as single atoms. Temperature dependent crystallographic studies of the structure from 100–500 K indicate that the CDW is “locked in”. Electrical conductivity and thermopower measurements in the temperature range of 300–500 K show that $\text{YCo}_{0.88}\text{Ga}_3\text{Ge}$ is a poor metal.

Introduction

Compounds with charge density waves (CDWs) have the potential to exhibit unusual properties including large dielectric constants, non-ohmic electrical resistivity, and elastic softening.^{1–3} CDWs form when electrons and phonons couple and depart from a uniform distribution, creating periodic regions of high and low electron density; they may or may not be commensurate with the periodicity of the lattice atoms. This modulated arrangement commonly becomes favorable when electrons are confined to low-dimensional structures, such as chains and layers.

Accurately determining the structures of CDW compounds remains a major challenge. It is often difficult to see the modulations with X-rays and sometimes is necessary to use techniques such as selected area electron diffraction (SAED). When the modulation can be observed with careful X-ray examinations, the structure can then be determined, but requires advanced superspace crystallographic techniques. The modulated structures for a series of RETe_3 (RE = rare earth element) as well as RESeTe_2 compounds have been successfully determined.^{4–6} The factors that can significantly affect the CDWs include changes in electronic structure and

configuration, pressure, temperature, and impurities. Chemical substitutions on the RE site in RETe_3 compounds for different RE atoms do not significantly change the valence electronic configuration of the RETe_3 compounds, which are essentially isoelectronic if it is assumed that the RE atom only donates three valence electrons. RE substitution, however, reveals that the modulation pattern found in the tellurium nets does vary with changes in RE atom possibly because of “chemical pressure” effects.⁷ CDW behavior has been found in several intermetallic compounds including: $\text{RE}_5\text{M}_4\text{Si}_{10}$ (M = Ir, Rh), LaAgSb_2 , and MRuSi (M = Zr, Hf).^{8–11} Thorough structural investigations into intermetallic CDW systems remain sparse.

Recently, the first modulation in gallium square nets was observed in $\text{RECo}_{1-x}\text{Ga}_3\text{Ge}$ type compounds where RE =

* To whom correspondence should be addressed. E-mail: m-kanatzidis@northwestern.edu.

- (1) Blumberg, G.; Littlewood, P.; Gozar, A.; Dennis, B. S.; Motoyama, N.; Eisaki, H.; Uchida, S. *Science* **2002**, *297*, 584–587.
- (2) Gill, J. C. *J. Phys. F: Metal Phys.* **1980**, *10*, L81–L87.
- (3) Brill, J. W.; Zhan, X.; Staresinic, D.; Borovac, A.; Biljakovic, K. *J. Phys. IV France* **2002**, *12*, 283.
- (4) Fokwa Tsinde, B. P.; Doert, T. *Solid State Sci.* **2005**, *7*, 573–587.

- (5) Malliakas, C.; Billinge, S. J. L.; Kim, H. J.; Kanatzidis, M. G. *J. Am. Chem. Soc.* **2005**, *127*, 6510–6511.
- (6) Malliakas, C. D.; Kanatzidis, M. G. *J. Am. Chem. Soc.* **2006**, *128*, 12612–12613.
- (7) DiMasi, E.; Aronson, M. C.; Mansfield, J. F.; Foran, B.; Lee, S. *Phys. Rev.* **1995**, *B52*, 14516–14525.
- (8) Lue, C. S.; Hsu, F. H.; Li, H. H.; Yang, H. D.; Kuo, Y.-K. *Physica C* **2001**, *364–365*, 243–246.
- (9) Seo, D.-K.; Ren, J.; Whangbo, M.-H.; Canadell, E. *Inorg. Chem.* **1997**, *36*, 6058–6063.
- (10) Song, C.; Park, J.; Koo, J.; Lee, K.-B.; Rhee, J. Y.; Bud'ko, S. L.; Canfield, P. C.; Harmon, B. N.; Goldman, A. I. *Phys. Rev.* **2003**, *B68*, 035113–1–035113–6.
- (11) Van Smaalen, S.; Shaz, M.; Palatinus, L.; Daniels, P.; Galli, F.; Nieuwenhuys, G. J.; Mydosh, J. A. *Phys. Rev.* **2004**, *B69*, 014103–1–014103–11.

Gd and Sm with SAED.¹² Subsequently, the modulated structure for GdCo_{0.88}Ga₃Ge was determined using super-space crystallographic techniques at 293 K.¹³ The CDW structurally manifested itself in the Ga net as a series of rows of single atoms, zigzag chains, and the occasional ribbon that run perpendicular to the *a*-axis. To understand how the CDWs in the RECo_{1-x}Ga₃Ge system behave, it is necessary to investigate and compare the CDWs in other RE analogues. Here we investigate the effects of a small electronic perturbation to the CDW by solving the modulated structure of YCo_{0.88}Ga₃Ge. We find that the yttrium compound has a different and unique distortion. In addition, we report the first temperature dependent study of a CDW in a Ga square net and the electronic properties of YCo_{0.88}Ga₃Ge.

Experimental Details

Synthesis of YCo_{0.88}Ga₃Ge. Molten Ga was used as a solvent to prepare the intermetallic compound YCo_{0.88}Ga₃Ge. Y powder (99.9%, Aldrich), Co powder (99.9+%, Aldrich), and Ga pieces (99.999%, Plasmaterials) were used as obtained. The Ge pieces (99.99%, Plasmaterials) were ground into a powder and then used. 1.5 mmol Y, 0.75 mmol Co, 11.2 mmol Ga, and 0.75 mmol Ge were loaded into alumina crucibles in a nitrogen filled glovebox. The crucibles were placed into fused silica tubes, evacuated to approximately 7×10^{-4} Torr, and flame sealed. The reactions were then placed in a furnace and treated with the following heating profile: the temperature was raised to 1273 K at 56 K/h and held at 1273 K for 5 h to ensure proper melt, then the temperature was cooled to 1123 K in 2 h and kept isothermally at 1123 K for 36 h, and then the temperature was cooled to 523 K at 100 K/h.

The products were separated from the excess molten flux by centrifuging the liquid Ga through a coarse frit at ~523 K. The products were further isolated from the Ga by soaking them in a 3 M solution of iodine in dimethylformamide (DMF) over a 36 h period. Any residual Ga was converted to GaI₃. The resulting crystalline products were rinsed with alternating portions of DMF and hot deionized water until the filtrate ran colorless. Then the products were dried with acetone. The silver metallic compound YCo_{0.88}Ga₃Ge crystallizes with square plate morphology and was recovered in approximately 60–80 wt % yields.

Structure Determination. Single-crystal X-ray diffraction data were collected with the use of graphite-monochromatized Mo K α radiation ($\lambda = 0.71073$ Å) at 100, 293, 400, and 500 K on a STOE IPDS II diffractometer. Data were collected by 1° scans in ω at a ϕ setting of 0°. Several crystals were tested for quality. Because the *q* vector length at any given temperature did not significantly change from crystal to crystal, only the best refinements are presented here. The collection of intensity data, data reduction, and numerical face-indexed absorption corrections were carried out with the XAREA program package.¹⁴ Refinements of the crystal structure were carried out with the Jana2000 program.¹⁵ Analysis of the reflections in reciprocal space revealed two categories of reflections: (1) strong intensity Bragg reflections that could be indexed to a tetragonal cell and (2) additional vectors of weaker intensity at

locations incommensurate with the tetragonal lattice. The following refinement was used for the data collected at 293 K; however, the same refinement strategy was used for each data set refinement. The lattice parameters were least-squares refined from the positions of 3071 reflections and a (3 + 1)D indexing: $a_s = 4.1639(4)$ Å, $c_s = 23.541(2)$ Å, $\mathbf{q} = 0.3200\mathbf{a}^*$, and $V_s = 408.16(7)$ Å³ ($Z = 4$).

Analysis of reciprocal space reveals weak satellite reflections in both *a** and *b** directions. A classical (3 + 2)D processing within the tetragonal symmetry (*I4/mmm*), however, does not describe the true aperiodic structure of the compound. This conclusion was supported by both the absence of cross term reflections (for example there were no $hklq_1q_2$ 1 0 0 1 1 reflections observed) and the presence of splitting of the Bragg reflections. Instead of a (3 + 2)D model, an orthorhombic (3 + 1)D superspace model with a simple twin whereby the *a* and *b* axes with similar cell constants exchange can be used to model YCo_{0.88}Ga₃Ge. A final data set merged according to the (mmm, 111) (3 + 1)D point group consisted of 8036 reflections (5597 observed) yielding an internal *R* value of 0.0465 for observed reflections ($I \geq 3\sigma(I)$ cutoff, redundancy of 6.225). The most probable superspace group was identified as *Immm*($\alpha 00$)00s from the systematic absences. Initially, the main Bragg reflections were used to establish a tetragonal disordered structure. Upon conversion of the tetragonal structure to orthorhombic symmetry, the residual *R* value for the observed reflections drops from 0.0470 (tetragonal symmetry, 22 parameters, 273 observed reflections) to 0.0255 (orthorhombic symmetry, 33 parameters, 442 observed reflections) with a convergence of the twin fraction to a 49/51 ratio. Despite the marked improvement on the residual *R* value, the atomic displacement parameter for Ga3 did not improve significantly (tetragonal symmetry, $U_{eq} = 0.029$; orthorhombic symmetry, $U_{eq} = 0.027$). The 3D structure does not reveal the true nature of the long-range ordering of the partial occupancies of Co2 and the two Ge sites (when Co2 and Ge2 are present Ge1 is not) suggested by the presence of satellite reflections.

Classical harmonic functions were added to the positional displacements of all the atoms as well as the occupational ordering of the Co2 and Ge sites. The resultant residual *R* value was 0.0497 for the observed reflections using 67 parameters and 1051 reflections. Close inspection of the residues around the Ga3 as a function of the internal *t* parameter suggested a better model for the thermal displacement parameters would be achieved with the addition of a third order Gram–Charlier nonharmonic development of the Debye–Waller factor for Ga3.^{16,17} Including the Debye–Waller factor for Ga3 and introducing a secondary extinction coefficient¹⁸ improved the refinement to a final residual value of $R = 0.0418$ ($R_w = 0.1176$) for 70 parameters. The final model included first order modulation waves on the positions of all the atoms, restrained first order modulation waves on the Co2, Ge1, and Ge2 atoms (the occupational modulation waves for Co2 and Ge2 are complimentary to that of Ge1), Debye–Waller factor modulation up to the first order for Ga3, and first order waves on the thermal displacement parameters of Y1, Co1, Ga1, Ga2, and Ga3. The thermal displacement parameters for Co2, Ge1, and Ge2 were not modulated because they became nonpositive definites upon convergence of the refinement.

Although the initial classical harmonic functions model yielded a reasonable residual *R* value of 0.0491 for 67 parameters, the final model including the Debye–Waller factor significantly improved the refinement to a final residual of $R = 0.0418$ for 70 parameters.

(12) Zhuravleva, M. A.; Pcionek, R. J.; Wang, X.; Schultz, A. J.; Kanatzidis, M. G. *Inorg. Chem.* **2003**, *42*, 6412–6424.

(13) Zhuravleva, M. A.; Evain, M.; Vaclav, P.; Kanatzidis, M. G. *J. Am. Chem. Soc.* **2007**, *129*, 3082–3083.

(14) X-Area, Version 1.39; STOE & Cie GmbH: Darmstadt, Germany, 2006.

(15) Petříček, V.; Dusek, M. *JAN A 2000*; Academy of Sciences of the Czech Republic: Prague, 2000.

(16) Johnson, C. K.; Levy, H. A. In *International Tables for Crystallography*; Ibers, J. A., Hamilton, W. C., Eds.; Kynoch Press: Birmingham, 1974; Vol. IV, pp 311–336.

(17) Kuhs, W. F. *Acta Cryst. A* **1984**, *40*, 133–137.

Table 1. Crystal Data and Structure Refinement for $\text{YCo}_{0.88}\text{Ga}_3\text{Ge}$ at 100, 293, 400, and 500 K

Crystal color	Metallic			
Crystal System	Orthorhombic			
Superspace group	$Immm(a00)00s$			
Temperature (K)	100	293	400	500
Formula	$\text{YCo}_{0.87}\text{Ga}_3\text{Ge}$	$\text{YCo}_{0.88}\text{Ga}_3\text{Ge}$	$\text{YCo}_{0.87}\text{Ga}_3\text{Ge}$	$\text{YCo}_{0.88}\text{Ga}_3\text{Ge}$
Molecular weight (g.mol ⁻¹)	422.0	422.5	422.0	422.5
Cell parameters				
<i>a</i> (Å)	4.1600(6)	4.1639(4)	4.1741(4)	4.1773(3)
<i>c</i> (Å)	23.522(3)	23.541(2)	23.578(3)	23.618(2)
<i>q</i> = <i>xa</i> *	0.3183(4)	0.3200(4)	0.3190(4)	0.3199(3)
<i>V</i> (Å ³)	407.06(9)	408.16(7)	410.80(8)	412.12(5)
<i>Z</i>	4	4	4	4
Density (calc., g.cm ⁻³)	6.8825	6.8736	6.8198	6.8074
Crystal description	Plate 1	Plate 2	Plate 3	Plate 3
Crystal size (mm ³)	0.215 x 0.140 x 0.020	0.201 x 0.162 x 0.066	0.183 x 0.162 x 0.015	0.183 x 0.162 x 0.015
hkl range	-5 ≤ <i>h</i> ≤ 5 -5 ≤ <i>k</i> ≤ 5 -32 ≤ <i>l</i> ≤ 32 -1 ≤ <i>m</i> ≤ 1	-6 ≤ <i>h</i> ≤ 6 -5 ≤ <i>k</i> ≤ 5 -36 ≤ <i>l</i> ≤ 36 -1 ≤ <i>m</i> ≤ 1	-6 ≤ <i>h</i> ≤ 6 -6 ≤ <i>k</i> ≤ 6 -37 ≤ <i>l</i> ≤ 37 -1 ≤ <i>m</i> ≤ 1	-7 ≤ <i>h</i> ≤ 7 -6 ≤ <i>k</i> ≤ 6 -38 ≤ <i>l</i> ≤ 37 -1 ≤ <i>m</i> ≤ 1
Twin matrices	$\begin{pmatrix} 1 & 0 & 0 \\ 0 & 1 & 0 \\ 0 & 0 & 1 \end{pmatrix} \begin{pmatrix} 0 & 1 & 0 \\ 1 & 0 & 0 \\ 0 & 0 & -1 \end{pmatrix}$			
Twin fractions	0.7779/0.2223	0.4947/0.5053	0.4954/0.5046	0.4852/0.5148
Linear absorption coeff (mm ⁻¹)	44.189	48.610	43.786	43.685
Overall $R(F)^a/R_w(F_o^2)^b$	0.0285/0.0793	0.0418/0.1176	0.0579/0.1290	0.0738/0.1785
Main reflections $R(F)^a/R_w(F_o^2)^b$	0.0174/0.0512	0.0315/0.0951	0.0406/0.0968	0.0682/0.1655
1 st Order reflections $R(F)^a/R_w(F_o^2)^b$	0.0743/0.1320	0.0641/0.1406	0.0981/0.1743	0.0904/0.1989
S(obs)/S(all)	1.36/1.43	2.08/2.25	1.89/2.04	2.90/3.23
No. of refined parameters	76	76	75	75
Secondary extinction coefficient	0.0010(1)	0.0016(3)	n/a	n/a
Difference Fourier residues (e ⁻ /Å ³)	[3.90, -3.70]	[3.25, -3.12]	[6.91, -5.29]	[4.05, -3.15]

^a $R(F) = \sum ||F_o| - |F_c|| / \sum |F_o|$ for $F_o^2 > 3\sigma(F_o^2)$.

^b $R_w(F_o^2) = [\sum w(F_o^2 - F_c^2)^2 / \sum wF_o^4]^{1/2}$, $w = 1/(\sigma^2(F_o^2) + 0.0016(F_o^2))$ for $F_o^2 \geq 3\sigma(F_o^2)$.

Data collected at 100, 400, and 500 K were modeled and refined in the same manner as the 273 K data. Crystallographic and refinement details are listed in Table 1 for data collected at 100, 273, 400, and 500 K. Details for the structure model refined from data collected at 273 K are presented in Tables 2–6; a complete set of tables for data sets collected at all temperatures are available in the Supporting Information. Tables 2–6 list the following: fractional atomic coordinates, their Fourier series modulation terms, and equivalent isotropic displacement parameters; occupation factors and their Fourier series modulation terms; anisotropic displacement parameters U^{ij} and their Fourier series modulation terms; selected distances and distance ranges; and Gram–Charlier nonharmonic Debye–Waller parameters C^{ijk} and their Fourier series modulation terms, respectively.

Thermopower Measurement. A Seebeck Measurement System (SMS) from MMR Technologies Inc. equipped with an SB-100 Seebeck controller and a K-20 programmable temperature controller was employed to measure the thermopower of several handpicked crystals of $\text{YCo}_{0.88}\text{Ga}_3\text{Ge}$. The SMS uses a comparative method to determine the thermopower of an unknown material relative to the thermopower of a known reference material. Here constantan was

used as the reference material. The thermopower for each crystal was measured over the temperature range of 310 to 500 K.

Conductivity Measurement. A home-built 4-probe high temperature (300–700 K) dc conductivity measurement system was used to measure the conductivity of single crystals of $\text{YCo}_{0.88}\text{Ga}_3\text{Ge}$ over a temperature range of 300–500 K. The 4-probe conductivity system is built from an altered Van der Pauw measurement system from MMR Technologies Inc. with a K-20 programmable temperature controller, a Keithley 2182A nanovoltmeter, a Keithley 6220 precision current source, and computer interface. The system measures the resulting voltage between two leads with an applied dc current from –50 to 50 mA at each temperature. The resistance is then extrapolated from the linear slope of each voltage versus current measurement. Then the conductivity can be calculated from the resistance, distance between voltage probes (*L*), and the cross sectional area (*A*). The dimensions, *A* and *L*, of each crystal were measured on a Hitachi S-3400N-II scanning electron microscope. Crystal 1, *L* = 0.0193 cm, *A* = 0.00106 cm²; Crystal 2, *L* = 0.0391 cm, *A* = 0.00458 cm².

(18) Becker, P. J.; Coppens, P. *Acta Crystallogr.* **1974**, *A30*, 129–147.

Table 2. Fractional Atomic Coordinates, Their Fourier Series Modulation Terms^a, and Equivalent Isotropic Displacement Parameters (Å²) for YCo_{0.88}Ga₃Ge Measured at 293 K

atom	wave	x	y	z	U _{eq}
Y1	0	0	0	0.14879(3)	0.0097(2)
	s,1	0	0	0.00009(4)	
	c,1	0.0321(3)	0	0	
Ga1	0	0	0.5	0.05476(5)	0.0113(3)
	s,1	0	0	-0.00262(5)	
	c,1	-0.0169(3)	0	0	
Ga2	0	-0.5	0	0.05456(5)	0.0108(3)
	s,1	0	0	-0.00504(7)	
	c,1	0.0094(2)	0	0	
Ga3	0	0	0.5	0.24673(15)	0.0206(4)
	s,1	0	0	0.00467(14)	
	c,1	-0.0455(8)	0	0	
Co1	0	0	0	0	0.0080(5)
	s,1	0	0	-0.00372(8)	
	c,1	0	0	0	
Co2	0	0	0	0.2779(6)	0.0108(6)
	s,1	0	0	-0.0023(8)	
	c,1	0.0098(7)	0	0	
Ge1	0	0	0	0.35625(15)	0.0140(4)
	s,1	0	0	-0.0013(2)	
	c,1	-0.0190(4)	0	0	
Ge2	0	0	0	0.3737(5)	0.0085(5)
	s,1	0	0	-0.0046(7)	
	c,1	-0.0079(6)	0	0	

^a The modulation for parameter λ of an atom ν is classically written as $U_{\nu}^{\lambda}(\bar{x}_4) = U_{\nu,0}^{\lambda} + \sum_{n=1}^k U_{\nu,s,n}^{\lambda} \sin(2\pi\bar{x}_4) + \sum_{n=1}^k U_{\nu,c,n}^{\lambda} \cos(2\pi\bar{x}_4)$.

Table 3. Occupation Factors and Their Fourier Series Modulation Terms^a for YCo_{0.88}Ga₃Ge Measured at 293 K

atom	wave	occupation
Co2	0	0.3768(3)
	s,1	-0.466(6)
	c,1	0
Ge1	0	0.6232(3)
	s,1	0.466(6)
	c,1	0
Ge2	0	0.3768(3)
	s,1	-0.466(6)
	c,1	0

^a The modulation for parameter λ of an atom ν is classically written as $U_{\nu}^{\lambda}(\bar{x}_4) = U_{\nu,0}^{\lambda} + \sum_{n=1}^k U_{\nu,s,n}^{\lambda} \sin(2\pi\bar{x}_4) + \sum_{n=1}^k U_{\nu,c,n}^{\lambda} \cos(2\pi\bar{x}_4)$.

Results and Discussion

Synthesis. YCo_{0.88}Ga₃Ge was synthesized using the gallium flux method at 1273 K. Large silver metallic crystals were obtained in 60–80 wt % yields. In an attempt to synthesize the other YCo_{1-x}Ga₃Ge stoichiometries, several different ratios of Y/Co were used. Reactions with larger Co amounts resulted in products of the off stoichiometric YCo_{0.88}Ga₃Ge and excess CoGa₃. Reactions with higher Y content only showed higher yields of YCo_{0.88}Ga₃Ge with respect to the Co content. No gallium flux reactions yielded crystals whose stoichiometry deviated significantly from YCo_{0.88(3)}Ga₃Ge.

Structure. Using conventional X-ray diffraction methods the entire RECo_{0.86(4)}Ga₃Ge (RE = Y, Sm, Gd, and Er) series appears to be isotypic, crystallizing in the tetragonal space group *I4/mmm*. Previously single crystal neutron diffraction studies were performed on YCo_{1-x}Ga₃Ge to conclusively determine the Ga and Ge positions,¹² the same assignments were used in the refinements presented here. Looking at the tetragonal subcell, one finds that there are two significant problems: (1) there is disorder between the Ge and Co sites

Table 4. Anisotropic Displacement Parameters U^{ij} (Å²) and Their Fourier Series Modulation Terms^a for YCo_{0.88}Ga₃Ge Measured at 293 K

atom	wave	U ¹¹	U ²²	U ³³	U ¹²	U ¹³	U ²³
Y1	0	0.0146(4)	0.0070(4)	0.0074(3)	0	0	0
	s,1	0.0052(3)	0.0002(5)	0.0004(3)	0	0	0
	c,1	0	0	0	0	0.0005(3)	0
Ga1	0	0.0181(6)	0.0060(5)	0.0099(5)	0	0	0
	s,1	0.0007(4)	-0.0001(7)	-0.0008(4)	0	0	0
	c,1	0	0	0	0	0.0006(3)	0
Ga2	0	0.0097(6)	0.0111(6)	0.0117(5)	0	0	0
	s,1	-0.0002(3)	-0.0007(7)	0.0024(5)	0	0	0
	c,1	0	0	0	0	0.0004(3)	0
Ga3	0	0.0291(7)	0.0153(8)	0.0175(5)	0	0	0
	s,1	0.0113(8)	0.0006(10)	0.0013(8)	0	0	0
	c,1	0	0	0	0	-0.0068(7)	0
Co1	0	0.0084(10)	0.0057(10)	0.0099(5)	0	0	0
	s,1	0	0	0	0	0	0
	c,1	0	0	0	0	0.0002(5)	0
Co2	0	0.0122(9)	0.0130(12)	0.0072(8)	0	0	0
Ge1	0	0.0129(6)	0.0077(8)	0.0214(8)	0	0	0
Ge2	0	0.0112(6)	0.0051(8)	0.0092(9)	0	0	0

^a The modulation for parameter λ of an atom ν is classically written as $U_{\nu}^{\lambda}(\bar{x}_4) = U_{\nu,0}^{\lambda} + \sum_{n=1}^k U_{\nu,s,n}^{\lambda} \sin(2\pi\bar{x}_4) + \sum_{n=1}^k U_{\nu,c,n}^{\lambda} \cos(2\pi\bar{x}_4)$.

Table 5. Gram–Charlier Non-Harmonic Debye–Waller Parameters C^{ijk} and Their Fourier Series Modulation Terms^b for YCo_{0.88}Ga₃Ge Measured at 293 K

atom	wave	C ¹¹¹	C ¹¹²	C ¹¹³	C ¹²²	C ¹²³
Ga3	0	0	0	-0.0058(5)	0	0
	s,1	0	0	-0.0071(7)	0	0
	c,1	0.079(10)	0	0	-0.015(4)	0
atom	wave	C ¹³³	C ²²²	C ²²³	C ²³³	C ³³³
Ga3	0	0	0	0.0017(5)	0	0.00006(3)
	s,1	0	0	-0.0007(7)	0	0.00004(3)
	c,1	0.00009(13)	0	0	0	0

^a C^{ijk} coefficients are multiplied 10^3 . ^b The modulation for parameter λ of an atom ν is classically written as $U_{\nu}^{\lambda}(\bar{x}_4) = U_{\nu,0}^{\lambda} + \sum_{n=1}^k U_{\nu,s,n}^{\lambda} \sin(2\pi\bar{x}_4) + \sum_{n=1}^k U_{\nu,c,n}^{\lambda} \cos(2\pi\bar{x}_4)$.

in between the Ga-net layer and the CoGa₄ slab (Figure 1), and (2) there are large thermal parameters on the Ga in the Ga-net layer. Careful analysis of the X-ray diffraction experiments indicated that the reciprocal lattice showed two types of reflections: (1) strong intensity Bragg reflections, and (2) spots of weaker intensity at locations incommensurate with the tetragonal lattice. Close inspection of the reflections revealed that the correct aperiodic structure was orthorhombic with pseudomerohedral twinning. Using a (3 + 1)D superspace approach the crystallographic least-squares refinements converged successfully once the tetragonal “subcell” model was reduced to orthorhombic symmetry and used as a starting model.^{19–22} At 293 K the modulation vector q of YCo_{0.88}Ga₃Ge was $0.3200(4)a^*$. From the systematic absences, *Immm*($\alpha 00$)00s (no. 71.b) was identified as the probable superspace group.^{16,17} A classical model with harmonic functions was employed to describe the modulation of the site occupancies of the Co/Ge disorder as well as the CDWs modulation in the Ga nets.

A fragment of the YCo_{0.88}Ga₃Ge as viewed down the [010] is shown in Figure 2A. An ordering of the site occupancies

(19) de Wolff, P. M. *Acta Crystallogr.* **1974**, *A30*, 777–785.

(20) Janssen, T.; Looijenga-Vos, A.; de Wolff, P. M. In *International Tables for Crystallography*; Wilson, A. J. C., Ed.; Kluwer Academic Publishers: Dordrecht, 1993; Vol. C, Chapter 9.8.

(21) Van Smaalen, S. Z. *Kristallogr.* **2004**, *219*, 681–691.

(22) Van Smaalen, S. *Cryst. Rev.* **1995**, *4*, 79–202.

Table 6. Main Distances (Å) $YCo_{0.88}Ga_3Ge$ Measured at 293 K^a

	average	minimum	maximum	Δ	multiplicity
Co1–Ga1	2.4493(9)	2.4353(13)	2.4624(13)	0.0271	× 4
Co1–Ga2	2.4477(11)	2.4092(10)	2.4855(10)	0.0763	× 4
Co2–Ge2	2.30(3)	2.275(19)	2.31(3)	0.035	× 1
Co2–Ga3	2.255(7)	2.235(5)	2.266(10)	0.031	× 2
	2.300(6)	2.189(5)	2.349(7)	0.160	× 2
Ge1–Ga1	2.931(3)	2.892(3)	3.011(3)	0.119	× 2
Ge1–Ga2	2.924(3)	2.894(4)	2.973(3)	0.079	× 2
Ge2–Ga1	2.678(10)	2.657(8)	2.700(8)	0.043	× 2
Ge2–Ga2	2.685(11)	2.682(8)	2.687(13)	0.005	× 2

^a Calculated on t intervals where atom occupancy is larger than 50%.

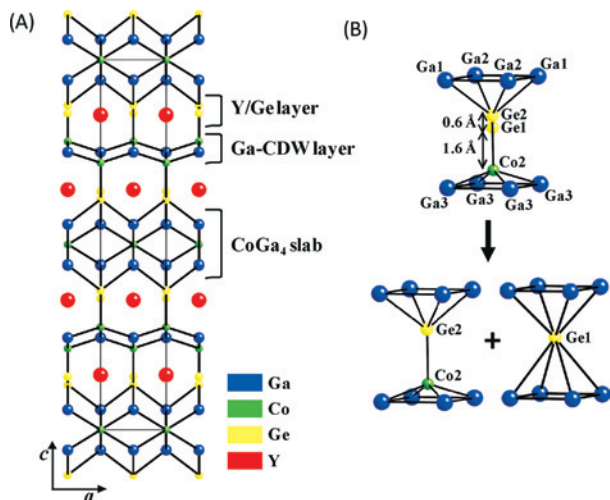


Figure 1. (A) Averaged structure of $YCo_{0.88}Ga_3Ge$ as viewed down the [010] (subcell). (B) Averaged coordination around the disordered Co2 and Ge1/Ge2 atoms and their breakdown of the two ordered environments in the modulated structure.

of the Co2–Ge2 and Ge1 positions can now be seen. The modulation of the CDW in the Ga net is shown in Figure 2B. For $YCo_{0.88}Ga_3Ge$ the modulation is manifested as infinite 1-D polygallide units. Rows of single atoms, zigzag chains, and ribbons run perpendicular to the a -axis creating an approximate 25-fold superstructure. The pattern of chains and ribbons in $YCo_{0.88}Ga_3Ge$ differs markedly from the pattern seen in $GdCo_{0.86}Ga_3Ge$ when using a cutoff of 2.93 Å for bond representations (Figures 2B and 2C, respectively). The CDW in $YCo_{0.88}Ga_3Ge$ consists of groups of ribbons separated by long segments of alternating chains and rows of single atoms, whereas in $GdCo_{0.86}Ga_3Ge$ it consists of single ribbons separated by segments of alternating zigzag chains and rows of single atoms. The divergence in patterns suggests that the electronic structure of the environment of the Ga-net plays a significant role in defining the CDW. In the substructure of $YCo_{0.88}Ga_3Ge$, the Ga–Ga distance is weakly nonbonding with the distance of about 2.94 Å in a perfect square net. The modulated structure, on the other hand, has Ga–Ga distances from 2.720(2)–3.198(3) Å for $YCo_{0.88}Ga_3Ge$. This is not nearly as drastic a deviation as seen in the Gd analogue. For $GdCo_{0.86}Ga_3Ge$ the Ga–Ga bonds were as short as 2.61 Å to approximately 3.2 Å. Therefore, the Ga-square net in the Y compound is not as distorted as the one in the Gd compound. One reason for this could be the smaller size of the Y, which exerts greater “chemical pressure” on the Ga net opposing the distortion. Chemical pressure can be understood in terms of distortions

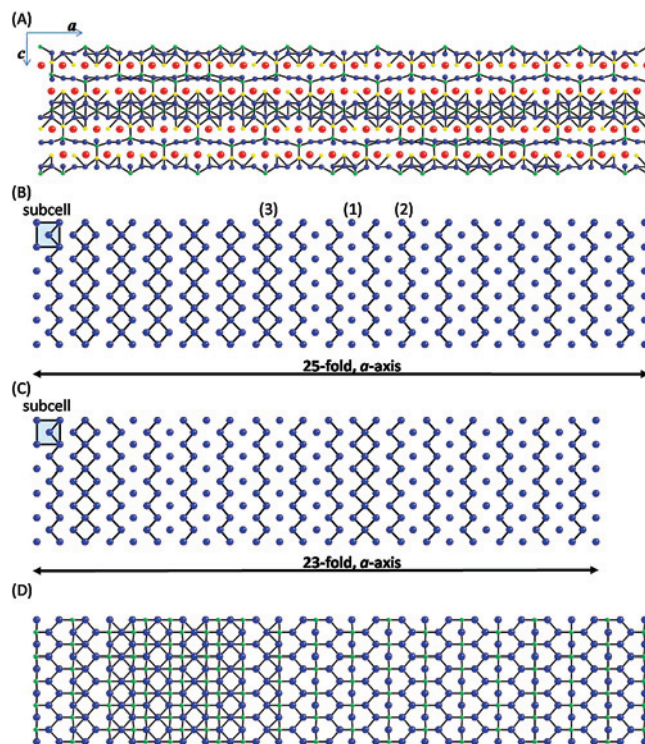


Figure 2. (A) Modulated, aperiodic structure of $YCo_{0.88}Ga_3Ge$ as viewed down the [010]. (Y, red; Co, green; Ga, blue; Ge, yellow) (B) CDW pattern in the Ga-net of $YCo_{0.88}Ga_3Ge$ as viewed down the [010]. The pattern is comprised of groups of rows of single atoms (1), zigzag chains (2), and ribbons (3). A Ga3–Ga3 distance cutoff of 2.93 Å was used for the bond representations. (C) CDW pattern in the Ga-net of $GdCo_{0.86}Ga_3Ge$ as viewed down the [010]. A Ga3–Ga3 distance cutoff of 2.93 Å was used for the bond representations. (D) CDW pattern in the Ga-net of $YCo_{0.88}Ga_3Ge$ with respect to the modulation of the Co2 occupancies. A Ga3–Ga3 distance cutoff of 2.93 Å was used for the bond representations and a greater than 50% occupancy limit was used to represent the presence of Co2. (data collected at 293 K).

induced by the size of the substituted RE atom. The unit cell contracts with chemical substitution in the same manner as if it were mechanically compressed. Because of the greater chemical pressure in the Y compound, the Ga net is prevented from distorting as much as it does in the Gd analogue.

In another comparison between the Y and Gd analogues the periodicity of the CDW is lengthened from approximately a 23-fold, a -axis superstructure for the Gd compound to approximately a 25-fold, a -axis superstructure for the Y compound. The Y and Gd analogues are isoelectronic; however, there are small changes in the electronic structure induced because of size effects.⁷ There are probably also small changes in the bonding orbital overlap associated with the d-orbitals of Y vis-à-vis Gd. Both the metal size and chemical bonding effects influence the density of states (DOS) $N(\epsilon_F)$ at the Fermi level (ϵ_F) by affecting band-width. These effects also influence ϵ_F itself. The CDW is highly dependent upon $N(\epsilon_F)$. In a simple metal the $N(\epsilon_F)$ is reduced when the cell volume decreases under pressure because the energy bands tend to broaden.

Conductivity and Thermopower. To search for any transitions in $YCo_{0.88}Ga_3Ge$ associated with suppression of the CDW, temperature dependent studies of its electrical properties were performed. Electrical conductivity and ther-

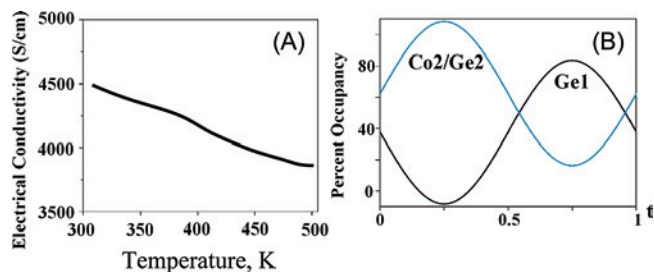


Figure 3. (A) Electrical conductivity of $\text{YCo}_{0.88}\text{Ga}_3\text{Ge}$ with temperature. (B) Site occupancy wave for Co2/Ge2 and Ge1 (data collected at 293 K).

mopower measurements were made on single crystals from 300–500 K parallel to the direction of the CDW. The thermopower remained relatively constant with the temperature having an average value of $\sim 8.0(6) \mu\text{V}/\text{K}$, indicating p-type charge transport. The conductivity decreases slowly from $\sim 4400 \text{ S}/\text{cm}$ at 300 K to $\sim 3900 \text{ S}/\text{cm}$ at 500 K in an almost linear fashion, Figure 3A. No transitions were observed over the measurement's temperature range. Attempts were made to measure the conductivity to higher temperatures (700 K); however, the $\text{YCo}_{0.88}\text{Ga}_3\text{Ge}$ reacts with the silver paste used to attach the leads to the crystals between 500 and 600 K resulting in odd electrical behavior. The magnitude of the conductivity is only moderate for an intermetallic compound and yet it is high enough to conclude that there is no full energy gap developed as a result of the CDW. As in the RETe_3 family the CDW distortion appears to remove a significant fraction of the DOS from the ε_{F} , but not all. This results in a poor metal but not a semiconductor.

Temperature Dependent X-ray Diffraction. To further probe into the nature of the CDW in $\text{YCo}_{0.88}\text{Ga}_3\text{Ge}$, X-ray diffraction studies were also performed at 100, 293, 400, and 500 K. The q-vector does not significantly change over the large temperature range ($q = 0.3183(4)a^*$, $0.3200(4)a^*$, $0.3190(4)a^*$, and $0.3199(3)a^*$ for 100, 293, 400, and 500 K respectively). Here, the argument for a decrease in stability of the CDW with decreasing cell volume does not hold true. In this range, the subcell volume goes from $407.06(9)$ to $412.12(5) \text{ \AA}^3$. The increase in volume would imply that the CDW, and therefore the q-vector, would increase in stability and become shorter. The CDW remains unchanged and appears “locked” into the most thermodynamically stable state, which is correlated to the site occupancy wave (SOW) modulation of the disordered Co2 site, Figure 3B. Figure 2D shows that the areas of high ribbon populations also have high populations of Co2 atoms, and where there are alternating chains and rows of single Ga atoms, only the rows of single Ga atoms have Co2 atom populations greater than 50% occupancy. The q-vector acts similarly to that in LaSeTe_2 where there is no change in q-vector length over the temperature range at which the CDW is present in the structure.²³ The apparent lack of a stoichiometric YCoGa_3Ge

phase also suggests that the CDW is highly coupled to the SOW of Co2 and is essential for the compound formation. Impurities are known to highly affect CDWs. Here ordered vacancies act as impurities and pin to the CDW. It is not known exactly which type of wave is formed first or which wave pins the other, but we can say that the coupling of the CDW and SOW is strong enough to prevent changes to the CDW that would normally be induced by temperature.

Conclusions

Initially YCoGa_3Ge and GdCoGa_3Ge were reported as isostructural compounds, but a close inspection of the modulated structures at 293 K reveals that the nature of the electropositive element (i.e., RE or Y) drastically changes the CDW frequency possibly because of bonding and size effects. As we inspect the modulation waves for $\text{YCo}_{0.88}\text{Ga}_3\text{Ge}$ with temperature, we find that the modulation frequency is “locked in” and does not significantly change within the error of the measurement. The CDW in the Ga square net seems to be sensitive to changes in RE element but also fixed to the SOW of Co2. To better understand the complicated mechanism regulating the CDW frequency and the role the SOW of the transition metal plays in these intermetallics additional RE analogs will have to be studied. The structural investigation of $\text{YCo}_{0.88}\text{Ga}_3\text{Ge}$ with temperature is essential for enabling and validating ab initio electronic structure calculations to deduce the causes of CDWs in these systems.

CDWs are believed to arise from electronic instabilities created by Fermi surface nesting. While we do not yet know if this nesting exists in the $\text{RECo}_{1-x}\text{Ga}_3\text{Ge}$ family, the CDW is associated with the square net of Ga. If we take into account that compounds with Te square nets invariably exhibit CDW behavior,^{4–6} we may have a general phenomenon where any square net of main group atoms is a potential source of a distortion.²⁴ This notion seems to be supported theoretically and will have to be verified experimentally by studying additional compounds with these structural features.²⁵

Acknowledgment. Financial support from the Department of Energy (DE-FG02-07ER46356) is gratefully acknowledged.

Supporting Information Available: Full tables of crystallographic data, refinements, and related information for $\text{YCo}_{0.88}\text{Ga}_3\text{Ge}$ collected at 100, 293, 400 and 500 K (PDF). This material is available free of charge via the Internet at <http://pubs.acs.org>.

IC801080F

(23) Doert, T.; Fokwa Tsinde, B. P.; Simon, P.; Lidin, S.; Söhnel, T. *Chem. Eu. J.* **2003**, *9*, 5865–5872.

(24) Patschke, R.; Kanatzidis, M. G. *Phys. Chem. Chem. Phys.* **2002**, *4*, 3266–3281.

(25) Papoian, G. A.; Hoffmann, R. *Angew. Chem., Intl. Ed.* **2000**, *39*, 2409–2448.